Avoided level crossings in very highly charged ions

P. Beiersdorfer,[*] J. H. Scofield, G. V. Brown, M. H. Chen, N. Hell,[†] A. L. Osterheld, D. A. Vogel,[‡] and K. L. Wong

Lawrence Livermore National Laboratory, Livermore, California 94550, USA

(Received 26 October 2015; published 13 May 2016)

We report a systematic measurement of the $(2p_{1/2}^{-1}3d_{3/2})_{J=1}$ and $(2s_{1/2}^{-1}3p_{1/2})_{J=1}$ levels in 14 neonlike ions between Ba^{46+} and Pb^{72+} and document the effects of their avoided crossing near $Z = 68$. Strong mixing affects the oscillator strengths over a surprisingly wide range of atomic numbers and leads to the vanishing of one transition two atomic numbers below the crossing. The crossing voids the otherwise correct expectation that the $(2p_{1/2}^{-1}3d_{3/2})_{J=1}$ level energy is only weakly affected by quantum electrodynamics (QED). For about 10 atomic numbers surrounding the crossing, its QED contributions are anomalously large, attaining almost equality to those affecting the $(2s_{1/2}^{-1}3p_{1/2})_{J=1}$ level. As a result, the accuracy of energy level calculations appears compromised near the crossing.

The diminishing importance of the Coulomb potential relative to relativistic and quantum electrodynamical (QED) effects, including the spin-orbit and spin-spin interactions, results in a marked rearrangement of the atomic structure along an isoelectronic sequence. The interchange proceeds smoothly for neighboring atomic levels with opposite parity or different angular momenta. The levels may "cross," i.e., they may have the same energy, and such crossings are of particular interest to parity violation experiments [1–4]. Because of the exclusion principle this is not the case, however, for two levels that have the same total angular momentum and the same parity. Quantum mechanical avoidance of such a crossing conflicts with the need for rearrangement of the atomic structure as the high-Z limit is approached and represents an obstacle for smooth restructuring [5]. Avoided crossings alter the radiative and autoionization rates along a given isoelectronic sequence [6–8] and may thus affect the choice of ionic systems used in the development of atomic clocks and the search of variations of the fine structure constant [9–11].

For ions of low charge the mixing of two levels typically occurs only for a very small, fractional range of atomic number Z, as shown computationally, for example, by Froese Fischer [12]. This means that effects associated with the crossing, other than the interchange of the two levels, may go unnoticed. For highly charged ions, calculations have shown that effects, such as on the radiative rates, extend over several adjoining ions [8,13,14]. Because levels appear to repel each other near the crossing, their energy values are also affected. Nakamura *et al.* presented calculations that yielded different contributions from QED terms depending on the calculational approach chosen to account for the strong configurational mixing associated with an avoided crossing [15]. They experimentally investigated the crossing of the $(2p_{1/2}^{-1}3s_{1/2})_{J=1}$ and $(2p_{3/2}^{-1}3d_{5/2})_{J=1}$ levels by measuring four neonlike ions between $Z = 53$ and 56. But these levels

were not strongly affected by QED, and the error limits of their measurements were too large to confirm the predictions. Moreover, the crossing did not considerably change the relative line intensities except for the fact that the line labels interchanged.

In the present Rapid Communication we focus on the crossing of a level that is strongly affected by QED with a level that—far from the crossing—is not. We have measured the level energies of 14 neonlike ions between Ba^{46+} and Pb^{72+} and find that the two levels share the QED energies in almost equal amounts near the crossing. This effect, attributable to strong mixing of the levels, allows us to distinguish even among subtle differences in the treatment of QED contributions. Such measurements thus provide a unique challenge for treating QED effects not afforded by measurements of noninteracting levels. We also find a very strong variation of the relative x-ray emission from the two levels over a large range of atomic numbers.

The 36 lowest excited levels in a neonlike ion have a vacancy in the $n=2$ shell and an optical electron in the $n=3$ shell. Our study focuses on the levels $(2p_{1/2}^{-1}3d_{3/2})_{J=1}$ and $(2s_{1/2}^{-1}3p_{1/2})_{J=1}$, which decay to the closed-shell $1s^2 2s^2 2p^6\,^1S_0$ neonlike ground state via an electric dipole transition. Here $2p_{1/2}^{-1}$ and $2s_{1/2}^{-1}$ denote a vacancy in the respective subshell. In standard notation [16–18], we label the transitions $3C$ and $3B$, respectively, and note that their x-ray energy E equals the level energy. Because of the $2s$ vacancy, QED contributions represent about 0.2% of the energy of line $3B$, i.e., between 8 and 35 eV for the range of Z of present interest. The QED contributions to line $3C$ are roughly an order of magnitude smaller.

In the low-Z limit, $E(3B) > E(3C)$ because the strength of the $2s$-binding energy exceeds that of the $2p$-binding energy. The energy ordering reverses in the high-Z, relativistic limit, as the $j=1/2$ electrons become more tightly bound than the $j=3/2$ electrons because of the diminishing importance of the electron-electron Coulomb potential relative to spin-orbit and spin-spin interactions, relativistic, and QED effects. Single- and multiconfiguration calculations of $E(3B)$ and $E(3C)$ with the Dirac-Fock code GRASP [19,20] are shown in Fig. 1(a). Results of the single-configuration calculation clearly indicate the energy reversal near $Z = 68$. Allowing for configuration mixing among the 36 excited levels, the interchange is less

_____

*beiersdorfer1@llnl.gov

[†]Also at Dr. Karl Remeis-Sternwarte and ECAP, Universität Erlangen-Nürnberg, 96049 Bamberg, Germany.

[‡]Present address: Middle Georgia State University, Macon, GA 31206, USA.
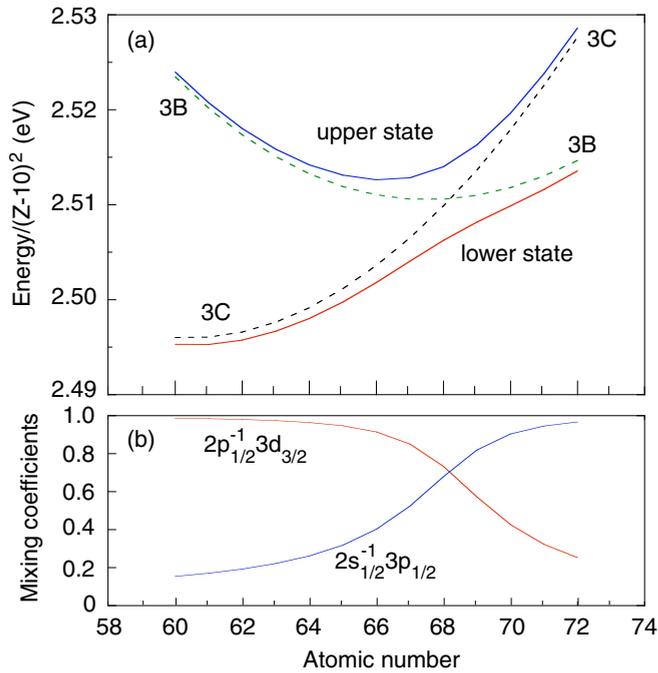
FIG. 1. (a) Predicted energies of levels $(2p_{1/2}^{-1}3d_{3/2})_{J=1}$ and $(2s_{1/2}^{-1}3p_{3/2})_{J=1}$, denoted $3C$ and $3B$, respectively. Dashed lines represent single-configuration calculations and the reversal in the energy ordering can be seen near $Z = 68$. Solid lines represent multi-configuration calculations. (b) The corresponding mixing coefficients for the lower level. The dominant components reverse near $Z = 68$.

obvious; the "upper" and "lower" levels approach each other, but diverge ("repel") near $Z = 68$. The interchange only becomes clear upon inspection of the mixing coefficients in Fig. 1(b), which shows that the dominant configurations making up the upper and lower levels reverse near $Z = 68$. As shown below, the amount of mixing and thus the actual interchange is uncertain within one atomic number in our calculations and depends on the type of calculation employed. The uncertainty spread in Z where the interchange happens is even larger in the literature [21,22]. In the following, we label the upper transition $3C$ for $Z \geqslant 68$ in accordance with the mixing coefficients calculated below in approach A2.

Measurements were made on the Livermore EBIT-I electron beam ion trap with a high-resolution von Hámos spectrometer [23,24]. The spectrometer employed a cylindrically bent LiF(200) or Si(220) crystal with a 30-cm radius of curvature, affording a resolving power of $\lambda/\Delta\lambda \approx 1800 - 2400$. The electron beam energy in all measurements was set to just below the ionization potential of the respective neonlike ion to maximize its abundance in the trap. The EBIT-I microcalorimeter [25,26] provided additional line intensity measurements.

Two representative L-shell spectra showing the transitions $3B$ and $3C$ in Er^{58+} and Yb^{60+} are displayed in Fig. 2. Near the interchange (i.e., Er^{58+}), mixing of the levels is largest, and the intensity of $3B$ approaches and exceeds that of $3C$. This behavior is in contrast to its low intensity far away from the crossing, where mixing with $3C$ is small, as shown in Fig. 3. The intensity ratio exhibits two additional
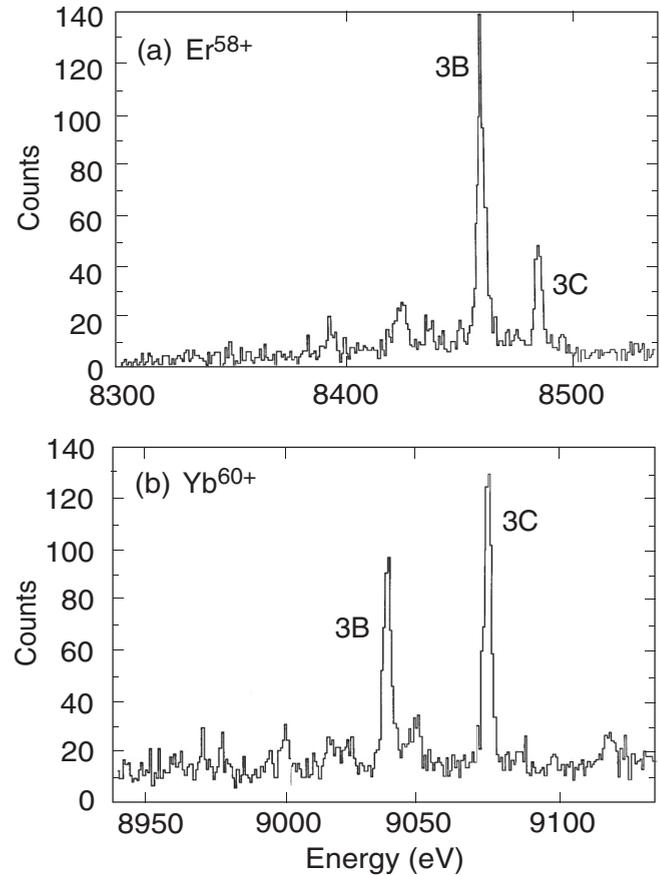
FIG. 2. L-shell spectra from Er^{58+} and Yb^{60+}. The two lines are labeled by their dominant components in accordance with Table I.

distinct features. First, the relative intensity of $3B$ is two to three times larger in the high-Z limit than in the low-Z limit. Second, line $3B$ virtually vanishes for $Z = 66$ (Dy^{56+}), i.e., several atomic numbers before the crossover. The latter is caused by a near vanishing of its oscillator strength and a corresponding drop in its radiative transition probability by several orders of magnitude, allowing $2s$-$2p$ intrashell
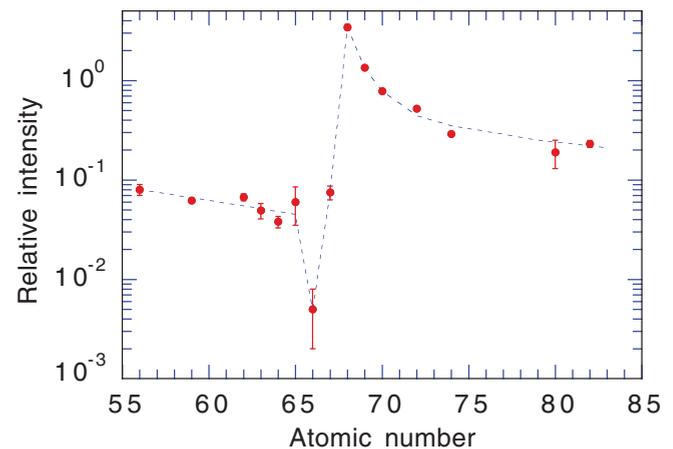
FIG. 3. Z-dependent intensity of line $3B$ relative to $3C$. Error bars are statistical. Note that the intensity of $3B$ exceeds that of $3C$ at the crossing and virtually vanishes for $Z = 66$.

transitions to effectively compete with the decay to the ground state. A similar intensity pattern was predicted in a study of level crossings in low-charge ions by Froese Fischer [12]. While Froese Fischer needed noninteger values of Z to calculate and exhibit vanishing and crossover, the interaction is so strong compared with the rate of change of the energy splitting in the present case that the perturbation extends over a finite range of ions, making experimental observation possible.

The energies of lines $3B$ and $3C$ were determined by intermittent recording of hydrogenlike and heliumlike K-shell reference spectra, similar to the procedures in Ref. [27]. For this, the wavelengths of the hydrogenlike Ly-α lines were set to the values calculated by Johnson and Soff [28]; those of the Ly-β,-γ,-δ, and -ϵ lines were set to the values calculated by Erickson [29]; and those of the heliumlike $^1P_1$ resonance line were set to the values calculated by Drake [30]. While there is no disagreement in the literature about the energy values of hydrogenlike ions [31], there is disagreement among the available energy values of the heliumlike ions, both calculated and measured [32,33]. The uncertainty in the heliumlike reference lines, however, is smaller than our measurement errors and does not affect our results. The particular reference transitions and the results of the measurement are listed in Table I. Data from Ref. [27] are also included. Errors are a combination of statistical and systematic uncertainties.

Our structure calculations were performed using the multiconfiguration Dirac-Fock (MCDF) codes of Grant *et al.* [19,20,34,35] by minimizing the average energy of all 36 singly excited levels in the $n = 3$ spectroscopic complex weighted by their respective statistical weights in the so-called extended-average-level (EAL) approach. The ground state was calculated separately in a single-configuration approximation. The calculations included the frequency-dependent Breit interaction as well as screened QED corrections and corrections

for residual correlation energies. The latter were estimated in a calculation that optimized each level separately in the so-called optimum level (OL) approach [19,20]: for $3B$ we included configuration interaction with the levels $(2s^2 2p^4 3p 3d)_{J=1}$ and $(2s^2 2p^4 3s 3p)_{J=1}$ to account for Coster-Kronig fluctuations; for $3C$ we included the $(2s^2 2p^5 4d)_{J=1}$ level to account for interactions with the nd Rydberg series. Residual correlations lowered the $3B$ energies by about 2 eV, except near the crossing where the Coster-Kronig corrections almost vanish; the correlations for $3C$ were small ($\leqslant 0.4$ eV). The QED corrections comprise vacuum polarization and self-energy terms that are estimated from screened hydrogenic values. Two differing ways are used to add the QED corrections to each level. In approach A1, the corrections are added *after* solving for the eigenfunctions and eigenvalues, using the procedure described by McKenzie *et al.* [35]. In approach A2, the QED corrections are applied to each orbital *before* diagonalization, using the procedure described by Dyall *et al.* [19].

The results from the two approaches, listed in Table I, are indistinguishable away from the crossover, implying that the two approaches are equivalent. Inspection near the crossover, however, reveals significant differences. Because the non-QED energies are virtually the same for each level in both approaches, as shown in Fig. 4, the differences must arise from the QED corrections. The values of the self-energy corrections for each level computed by the two approaches are shown in Fig. 4. Both approaches show that the crossing affects the apportionment of the self-energy contribution over about 10 atomic numbers.

An assessment of the accuracy of each calculation is given by Fig. 5 where we plot the difference between the predicted and measured level energies. The effect of the crossover is readily evident for $3C$ and manifests itself by a dip of about 2 eV (green trace) and 5 eV (blue trace) in the overall trend between $Z = 67$ and 72. The effect is not as clear for $3B$. The

TABLE I. Comparison of measured and calculated energies of lines $3B$ and $3C$. Theoretical energies are from MCDF calculations employing the two approaches discussed in the text. All values are in eV. Kα transitions in the hydrogenlike or heliumlike ions listed served as reference standards; exceptions are indicated by (Ryd), where Ly-β or transitions from higher n levels served as standards. No reliable energy measurement was possible for $3B$ of dysprosium or gold.

		$3B$			$3C$			Wavelength reference
	Z	E_{expt}	E_{theo}-A1	E_{theo}-A2	E_{expt}	E_{theo}-A1	E_{theo}-A2	
Ba	56	5381.17 ± 0.20	5381.94	5381.93	5295.20 ± 0.20	5295.21	5295.06	$V^{21+}, V^{22+}, Cr^{22+}$
Pr	59	6069.87 ± 0.30	6070.97	6070.97	5996.56 ± 0.20	5996.42	5996.29	Ti^{20+}, Ti^{21+}(Ryd)
Sm	62	6809.43 ± 0.20	6810.75	6810.69	6752.87 ± 0.15	6752.57	6752.48	Fe^{24+}, Fe^{25+}
Gd	64	7332.97 ± 0.40	7333.72	7333.56	7289.18 ± 0.40	7288.36	7288.39	Co^{25+}, Co^{26+}
Tb	65	7603.31 ± 1.20	7605.30	7604.96	7566.78 ± 1.00	7565.80	7566.00	Ni^{26+}, Ni^{27+}
Dy	66		7883.38	7882.64	7850.33 ± 0.10	7849.37	7849.97	Ni^{26+}, Ni^{27+}
Ho	67	8165.77 ± 0.65	8169.27	8167.66	8140.10 ± 0.40	8138.48	8139.94	Ni^{26+}, Ni^{27+}
Er	68	8434.06 ± 0.20	8432.49	8435.07	8459.76 ± 0.20	8463.71	8460.98	Cu^{27+}, Cu^{28+}
Tm	69	8733.61 ± 0.50	8732.12	8734.80	8762.60 ± 0.50	8766.21	8763.39	Cu^{27+}, Cu^{28+}
Yb	70	9038.93 ± 0.40	9037.39	9039.19	9076.19 ± 0.40	9077.09	9075.12	Zn^{28+}, Zn^{29+}
Hf	72	9665.06 ± 0.70	9664.42	9665.00	9725.76 ± 0.70	9725.15	9724.42	Ti^{20+}, Ti^{21+}
W	74	10317.23 ± 0.50[a]	10317.91	10318.14	10408.69 ± 0.40[a]	10407.80	10407.43	
Au	79		12079.23	12079.43	12270.91 ± 0.90	12267.94	12267.75	Mn^{23+}, Mn^{24+}
Hg	80	12454.36 ± 2.20	12455.19	12455.17	12671.75 ± 0.50	12667.82	12667.63	Ti^{20+}, Ti^{21+}(Ryd)
Pb	82	13230.95 ± 2.00	13231.76	13231.76	13500.43 ± 0.70	13497.38	13497.22	Fe^{24+}, Fe^{25+}

[a]Values from Ref. [27].
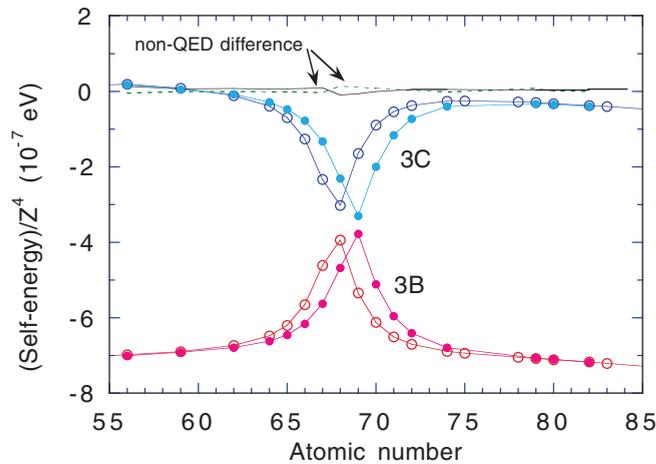
FIG. 4. Self-energies of levels $3B$ and $3C$ calculated with approach A1 (open circles) and approach A2 (solid circles) discussed in the text. The differences in the non-QED energies of the two levels calculated with the two procedures are shown for comparison.

indication of a dip (2.5 eV; blue trace) and of a shallow trough is seen below, that of a peak or rise is seen above the crossing. The effects of the crossover, thus, are generally less noticeable in the comparison with A2 (green trace) than with A1 (blue trace), indicating a more consistent agreement of this approach with the measurements.

In Fig. 5 we have also plotted the difference between our measured values and those predicted by Safronova *et al.* using second-order relativistic many-body perturbation theory (RMBPT; yellow trace) [14]. A clear, 2.5 eV dip is seen for $3B$. That dip, however, is shifted from those seen in the comparison with A1 and A2; instead it lines up with the dips seen for those approaches in $3C$. The differences for $3C$ show a discontinuity of the general positive and increasing trend at $Z = 67$, where the difference is negative (-0.8 eV), before rising to $+2.5$ at $Z = 68$.

To address the possibility that yet different amounts of mixing and thus apportionment of the QED energies may provide a better description of the data, we look at the sum energy $E(\text{sum}) = E(3B) + E(3C)$, which is invariant to the QED apportionment between the two levels. A comparison with the data is shown in Fig. 5. A pronounced dip is seen in our MCDF values at the crossing, where theory overestimates $E(\text{sum})$ by more than 2 eV ($Z = 67, 68, 69$); by contrast, just above the crossing theory underestimates the measured values ($Z = 70, 72$). Thus, having ruled out the uncertainty in the apportionment of the QED contribution, we find that the agreement between our calculations and the data does not significantly improve when considering the sum. This suggests that the calculated QED corrections themselves are significantly less accurate near the crossing than elsewhere. By contrast, the RMBPT results seem to do better up to $Z = 69$. Then there is a jump of 4 eV for $E(\text{sum})$ as the atomic number increases from $Z = 69$ and $Z = 70$. Moreover, the RMBPT results are in much worse agreement with experiment than the MCDF values for $Z \geqslant 70$, with the disagreement rising to more than 8 eV for $Z \geqslant 80$, which is too large to fit on the graph.

We summarize by noting that we have presented a systematic study of the effects of an avoided level crossing
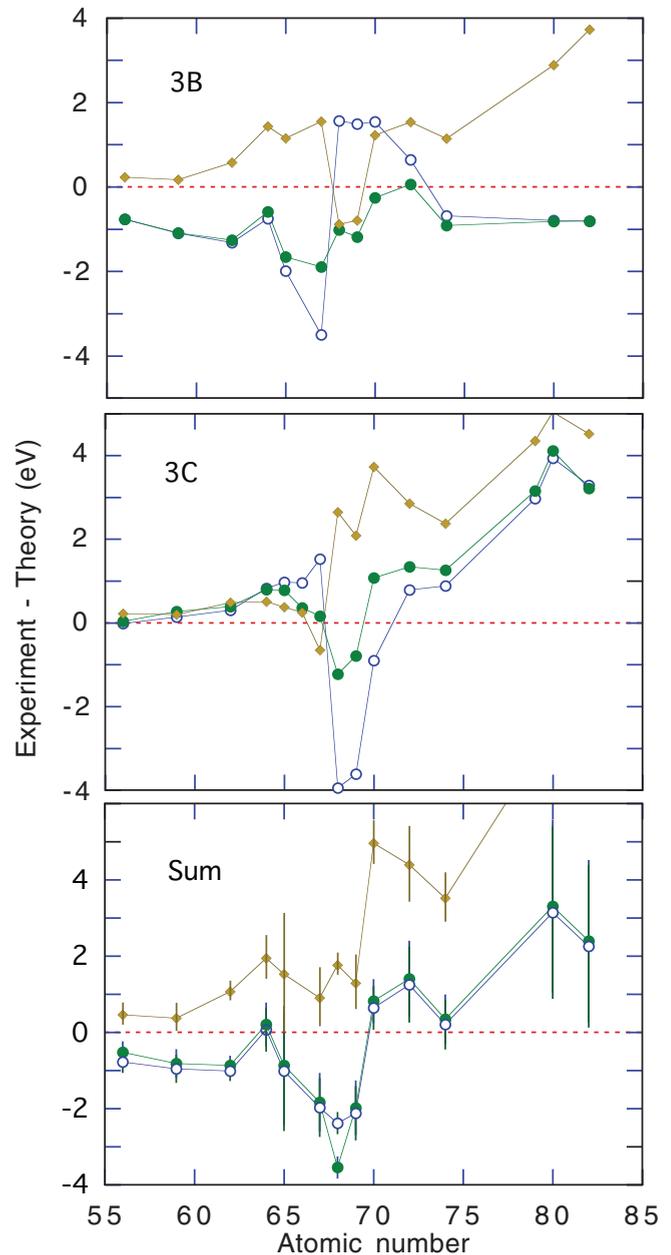
FIG. 5. Z-dependent differences between measured and calculated energies for lines $3B$ and $3C$, and their sum. Open blue (solid green) circles represent calculations using approach A1 (A2). RMBPT calculations are represented with solid yellow diamonds. Error limits represent the quadrature sum of the individual experimental uncertainties listed in Table I.

on the x-ray emission and level structure affected by strong QED contributions. The effects of the crossing are seen in the line intensities, which equalize at the crossing, but lead to a near vanishing of one of the lines two atomic numbers below the interchange. The uncertainty in accurately predicting the degree of mixing of the strongly interacting levels introduces a degree of arbitrariness in the apportionment of the QED energies derived from screened hydrogenic values. When the issue of apportionment is neutralized by studying only the summed energies we find that the calculated QED

values remain less reliable for a range of Z surrounding the crossing than farther away, although the RMBPT values seem to diverge from experiment more strongly than the MCDF values for $Z \geqslant 70$. Systematic studies of crossings of strongly interacting levels with disparate QED contributions thus appear to provide a test case for developing reliable energy level calculations not afforded by the more common QED measurements of noninteracting levels in hydrogenlike, lithiumlike, or sodiumlike high-Z ions.

[1] A. Schäfer, G. Soff, P. Indelicato, B. Müller, and W. Greiner, Phys. Rev. A **40**, 7362 (1989).

[2] M. Maul, A. Schäfer, W. Greiner, and P. Indelicato, Phys. Rev. A **53**, 3915 (1996).

[3] V. M. Shabaev, A. V. Volotka, C. Kozhuharov, G. Plunien, and T. Stöhlker, Phys. Rev. A **81**, 052102 (2010).

[4] F. Ferro, A. Artemyev, T. Stöhlker, and A. Surzhykov, Phys. Rev. A **81**, 062503 (2010).

[5] J. von Neumann and E. P. Wigner, Physikalische Zeitschrift **30**, 467 (1929).

[6] U. I. Safronova, W. R. Johnson, and A. E. Livingston, Phys. Rev. A **60**, 996 (1999).

[7] M. F. Hasoğlu, D. Nikolić, T. W. Gorczyca, S. T. Manson, M. H. Chen, and N. R. Badnell, Phys. Rev. A **78**, 032509 (2008).

[8] U. I. Safronova, A. S. Safronova, and P. Beiersdorfer, Phys. Rev. A **90**, 012519 (2014).

[9] J. C. Berengut, V. A. Dzuba, and V. V. Flambaum, Phys. Rev. Lett. **105**, 120801 (2010).

[10] J. C. Berengut, V. A. Dzuba, V. V. Flambaum, and A. Ong, Phys. Rev. Lett. **106**, 210802 (2011).

[11] M. S. Safronova, V. A. Dzuba, V. V. Flambaum, U. I. Safronova, S. G. Porsev, and M. G. Kozlov, Phys. Rev. Lett. **113**, 030801 (2014).

[12] C. Froese Fischer, Phys. Rev. A **22**, 551 (1980).

[13] P. Beiersdorfer, A. L. Osterheld, V. Decaux, and K. Widmann, Phys. Rev. Lett. **77**, 5353 (1996).

[14] U. I. Safronova, C. Namba, I. Murakami, W. R. Johnson, and M. S. Safronova, Phys. Rev. A **64**, 012507 (2001).

[15] N. Nakamura, D. Kato, and S. Ohtani, Phys. Rev. A **61**, 052510 (2000).

[16] J. H. Parkinson, Astron. Astrophys. **24**, 215 (1973).

[17] P. Beiersdorfer, S. von Goeler, M. Bitter, E. Hinnov, R. Bell, S. Bernabei, J. Felt, K. W. Hill, R. Hulse, J. Stevens, S. Suckewer, J. Timberlake, A. Wouters, M. H. Chen, J. H. Scofield, D. D. Dietrich, M. Gerassimenko, E. Silver, R. S. Walling, and P. L. Hagelstein, Phys. Rev. A **37**, 4153 (1988).

[18] P. Beiersdorfer, M. H. Chen, R. E. Marrs, and M. A. Levine, Phys. Rev. A **41**, 3453 (1990).

[19] K. G. Dyall, I. P. Grant, C. T. Johnson, F. A. Parpia, and E. P. Plummer, Comput. Phys. Commun. **55**, 425 (1989).

[20] F. A. Parpia, C. F. Fischer, and I. P. Grant, Comp. Phys. Comm. **94**, 249 (1996).

[21] T. Kagawa, Y. Honda, and S. Kiyokawa, Phys. Rev. A **44**, 7092 (1991).

[22] E. P. Ivanova and A. V. Gulov, At. Data Nucl. Data Tables **49**, 1 (1991).

[23] P. Beiersdorfer, R. E. Marrs, J. R. Henderson, D. A. Knapp, M. A. Levine, D. B. Platt, M. B. Schneider, D. A. Vogel, and K. L. Wong, Rev. Sci. Instrum. **61**, 2338 (1990).

[24] P. Beiersdorfer, Can. J. Phys. **86**, 1 (2008).

[25] F. S. Porter, G. V. Brown, K. R. Boyce, R. L. Kelley, C. A. Kilbourne, P. Beiersdorfer, H. Chen, S. Terracol, S. M. Kahn, and A. E. Szymkowiak, Rev. Sci. Instrum. **75**, 3772 (2004).

[26] F. S. Porter, B. R. Beck, P. Beiersdorfer, K. R. Boyce, G. V. Brown, H. Chen, J. Gygax, S. M. Kahn, R. L. Kelley, C. A. Kilbourne, E. Magee, and D. B. Thorn, Can. J. Phys. **86**, 231 (2008).

[27] P. Beiersdorfer, J. K. Lepson, M. B. Schneider, and M. P. Bode, Phys. Rev. A **86**, 012509 (2012).

[28] W. R. Johnson and G. Soff, At. Data Nucl. Data Tables **33**, 405 (1985).

[29] G. W. Erickson, J. Phys. Chem. Ref. Data **6**, 831 (1977).

[30] G. W. F. Drake, Can. J. Phys. **66**, 586 (1988).

[31] P. Beiersdorfer, Can. J. Phys. **87**, 9 (2009).

[32] P. Beiersdorfer, M. Bitter, S. von Goeler, and K. W. Hill, Phys. Rev. A **40**, 150 (1989).

[33] P. Beiersdorfer and G. V. Brown, Phys. Rev. A **91**, 032514 (2015).

[34] I. P. Grant, B. J. McKenzie, P. H. Norrington, D. F. Mayers, and N. C. Pyper, Comput. Phys. Commun. **21**, 207 (1980).

[35] B. J. McKenzie, I. P. Grant, and P. H. Norrington, Comput. Phys. Commun. **21**, 233 (1980).